Dynamics of Lake Eruptions and Possible Ocean Eruptions

Youxue Zhang[1,2] and George W. Kling[3]

[1]Key Laboratory of Orogenic Belts and Crustal Evolution, MOE, School of Earth and Space Sciences, Peking University, Beijing, 100871, China

[2]Department of Geological Sciences and [3]Department of Ecology and Evolution Biology, University of Michigan, Ann Arbor, Michigan 48109; email: youxue@umich.edu, gwk@umich.edu

Annu. Rev. Earth Planet. Sci.
2006. 34:293–324

First published online as a Review in Advance on January 16, 2006

The *Annual Review of Earth and Planetary Science* is online at earth.annualreviews.org

doi: 10.1146/annurev.earth.34.031405.125001

0084-6597/06/0530-0293$20.00

Key Words

gas-driven eruptions, lake eruptions, oceanic eruptions, natural hazards, mud craters, carbon sequestration

Abstract

Dissolved gas in liquid is able to power violent eruptions. Two kinds of such gas-driven eruptions are known in nature: explosive volcanic eruptions driven by dissolved H_2O in magma at high temperatures and lake eruptions driven by dissolved CO_2 in water at low temperatures. There are two known occurrences of lake eruptions, one in 1984 (Lake Monoun) and one in 1986 (Lake Nyos), both in Cameroon, Africa. The erupted CO_2 gas asphyxiated ~1700 people in the Lake Nyos eruption and 37 people at Lake Monoun. Here we review experimental simulations of CO_2-driven water eruptions and dynamic models of such eruptions, and a bubble plume theory is applied to the dynamics of lake eruptions. Field evidence, experimental results, and theoretical models show that lake eruptions can be violent, and theoretical calculations are consistent with the high exit velocities and eruption columns inferred from observations. Furthermore, the dynamics of lake degassing experiments are consistent with theoretical models. Other kinds of gas-driven eruptions are possible and may have occurred in nature in the past. A concentrated and large release of methane gas or hydrate from marine sediment may result in an ocean eruption. Furthermore, injection of liquid CO_2 into oceans might also lead to ocean eruptions if care is not taken. The various kinetic and dynamic processes involved are examined and quantified.

INTRODUCTION TO GAS-DRIVEN ERUPTIONS

No sight on Earth is more inspiring than that of an explosive volcanic eruption column ascending tremendously into the sky. Explosive eruptions are one kind of gas-driven eruptions, and they were the only kind known to science before 1984. Since that time, however, lake eruptions have been recognized (Freeth & Kay 1987; Kling et al. 1987, 1989; Sigurdsson et al. 1987; Sigvaldason 1989; Tazieff 1989; Freeth 1990; Freeth et al. 1990; Giggenbach 1990; Sabroux et al. 1990), and other types of gas-driven eruptions have been proposed (Chivas et al. 1987, Crawford & Stevenson 1988, Ryskin 2003, Zhang 2003). This paper reviews the dynamics of gas-driven eruptions, focusing on lake eruptions and possible ocean eruptions.

Gas-driven eruptions are powered by the rapid exsolution of initially dissolved gas in a liquid. At high system pressures, the gas component is dissolved in the liquid. As the system pressure decreases, the solubility of the gas in the liquid decreases. Once supersaturation of the gas is reached, bubbles nucleate and grow, leading to large volume expansion. The expansion either drives the bubbly liquid upward through a solid medium (as in volcanic eruptions), or leads to the buoyant rise of a bubble plume in a fluid medium (as in lake eruptions). The dynamics of gas-driven eruptions depend on the gas-liquid system, whether the eruption is through a solid conduit or a fluid medium, and the initial and boundary conditions.

Small-scale gas-driven eruptions may also be encountered during daily life. For example, champagne and beer may erupt when opened, especially if previously shaken. However, if opened carefully these liquids may not violently erupt because nucleation of bubbles is a difficult process. That is, for a system with a small degree of supersaturation, slow nucleation may suppress eruption. In such a case, addition of nucleation sites would facilitate eruptions. For example, if you enjoy beer and cigarettes (which we do not encourage), you may try the following "trick." Open a bottle of cold beer, without shaking it, and place it on a table. Although beer is oversaturated with CO_2, few bubbles would form and grow because nucleation requires some activation energy. Ask if your friends are able to drink it without touching the bottle by hand. When no one can accomplish this, light a cigarette and tap some cigarette ash into the beer. The ash particles provide nucleation sites and bubbles nucleate and grow. The resulting volume expansion drives bubbly beer to flow from the bottle mouth, where it can be consumed without touching the bottle.

Lake Eruptions

It might be a surprise that such large-scale geologic processes as lake eruptions were only recognized in the 1980s. After their discovery, the process and mechanisms puzzled scientists for some time. To date, there are only two known cases of lake eruptions, both from Cameroon, Africa, and only one other lake in the world, Lake Kivu in East Africa, is known to contain dangerous gas concentrations (Tietze et al. 1980, Kling et al. 1991). The eruption of Lake Monoun in August of 1984 killed ~37 people, and the eruption of Lake Nyos in August of 1986 killed ~1700 people up to 26 km away from the lake. The deaths led the lakes to be known as the "killer lakes."

Figure 1

Lake Nyos under normal conditions (May 1995) and after eruption (September 1986) (G. Kling). The change in surface color is due mainly to an iron-hydroxide that precipitated when anoxic bottom water rich in iron was mixed to the surface and oxidized during the eruption (Kling et al. 1987).

Eyewitnesses who were fortunate enough to survive the disaster gave the following account for Lake Nyos eruption (Kling et al. 1987). At about 21:30 they heard a series of rumbling or bubbling sounds lasting 15 to 20 seconds, and one observer walked to the crater rim and saw a white cloud or mist rise from the lake and a large water surge. Although people smelled the odor of rotten eggs or gunpowder, they lost consciousness owing to the lack of oxygen in the dense, ground-hugging cloud of CO_2 mixed with water vapor and droplets. Many animals also died in the Nyos eruption, but vegetation around the lake was not significantly affected. In addition, the surface of the lake turned reddish brown after the event owing to the oxidation of dissolved iron mixed to the surface from depth (**Figure 1**). At Lake Monoun, the eruption also occurred at night, and the gas cloud filled a low-lying area near the lake (Sigurdsson et al. 1987). Travelers on a nearby road were killed as they entered the area, as were people who left higher ground to help those who had fallen in the valley.

Ambioructic flow: term coined by Zhang (1996) to describe room-temperature CO_2 flow carrying water vapor and droplets, formed by the collapse of a lake eruption column. Ambioructic is formed by combining ambient and eruction. An eruction produces a CO_2 flow carrying water vapor and droplets

In the aftermath of the Lake Nyos disaster, many countries sent teams of scientists to investigate the cause of the disaster. The Cameroon Ministry of Higher Education and Scientific Research organized a conference in Yaoundé (the capital of Cameroon) in March 1987 on the cause of the Lake Nyos disaster. Two scientific hypotheses emerged from the conference about the origin of the massive CO_2 gas releases. The first was the volcanic hypothesis, in which a volcanic eruption occurred through the lake. The second was the limnic hypothesis, where gas was stored in the lake prior to the event and released during a lake overturn or mixing of surface and bottom waters. As evidence, scientists advancing the volcanic hypothesis cited the violence and localized nature of the process, color of the lake, smell of the gas, plus some other anecdotal evidence. However, surveys of the lake and surroundings failed to discover fresh volcanic rock, heat inputs to the lake, volcanic vents, or disturbed sediments (Kling et al. 1987). Whether these gas eruptions were volcanic in nature, and therefore impossible to stop, or whether they were limnological in nature, and therefore possible to identify and mitigate through gas removal, had direct political and socioeconomic consequences.

Considerable progress was made after the Yaoundé Conference in both the empirical understanding of the causes of the disasters and the theoretical understanding of CO_2-driven lake eruptions. Scientists now agree that the events were limnological in nature and represent CO_2-driven water eruptions owing to the rapid exsolution of CO_2 gas bubbles from dissolved CO_2 stored in the lakes. The basic processes of lake eruptions are as follows. Because the lakes overlie a volcanic field, CO_2 from magmas at depth gradually percolates upward through the overlying rocks and dissolves in near-surface groundwaters, which then enter the bottom of the lake as CO_2-charged springs [it is possible that free gas also enters the lakes, but this has never been demonstrated (Evans et al. 1993)]. As CO_2 dissolves in the lake bottom water, the density of water increases, which creates a stable stratification with less dense, CO_2-poor water at the lake surface. Further transport of CO_2 upward in the lake is controlled by diffusion. When CO_2 in bottom waters becomes oversaturated, bubbles nucleate and grow, leading to an erupting bubble plume. Even if CO_2 pressures are somewhat below saturation, an eruption could occur if there is an input of energy (such as a landslide) that moves bottom water upward to the point where dissolved gas pressure exceeds local hydrostatic pressure. There is still debate about the exact triggering mechanism (Cotel 1999) and the depth at which the eruption initiated (Evans et al. 1994).

After the erupting bubble plume exits the lake surface, the gas cloud eventually collapses and becomes a ground-hugging density flow because CO_2-rich gas is denser than air. Such a gravity current is similar to a pyroclastic flow. However, because the flow is not hot (pyro) and contains no clastic particles, Zhang (1996) coined the term ambioructic flow to describe the CO_2 flow carrying water droplets at ambient temperatures (ambioructic is formed by combining ambient and eruct; an eruction produces a water droplet–laden CO_2 flow). The CO_2-rich and O_2-poor density flow kills people and animals in its path through asphyxiation.

With this understanding of lake eruptions, mitigation measures are being taken to avoid future eruptions. An operational degassing pipe was installed in Lake Nyos

in 2001 and in Lake Monoun in 2003 (Halbwachs et al. 2004, Kling et al. 2005), although more pipes are needed to reduce the risk of future eruptions. It is hoped that the two known lake eruptions will be the only cases of lake eruptions.

Possible Ocean Eruptions

Although no one has observed or witnessed them yet, ocean eruptions have been hypothesized (Ryskin 2003, Zhang 2003). Enormous amounts of CH_4 are present in marine sediment in the forms of methane hydrate, methane gas, and dissolved methane in pore water (Kvenvolden 1988, 1998; Sloan 1990; Buffet 2000). The stability of the various forms of CH_4 can change when certain external conditions change, such as a rise in bottom water temperature (Dickens et al. 1995; Kennett et al. 2002), a drop in sea level (Paull et al. 1991), or a landslide or faulting (Bugge et al. 1987, Maslin et al. 1998, Rothwell et al. 1998). Such changes may cause a sudden conversion of methane hydrate to methane gas, generating overpressure in the gas-charged sediment and the eventual burst of methane gas. If a burst or other disturbance releases a large amount of CH_4 to seawater, either as gas or as hydrate that converts to gas, the gas could drive an eruption that in many ways is similar to a lake eruption. This methane-driven water eruption, not a fluidized sediment eruption, is referred to as an ocean eruption in this review. Ocean eruptions may provide a pathway for CH_4 in marine sediment to rapidly pass through the ocean water column to enter the atmosphere as a greenhouse gas.

Other Types of Eruptions

Other types of gas-driven eruptions have also been hypothesized. Crawford & Stevenson (1988) postulated that on the Jupiter satellite Europa, the temperature-depth profile is such that water at the surface is frozen but at depth can be liquid. In liquid water, carbon dioxide and other gases may be dissolved. This situation is similar to hydrous magma at depth in the Earth. As liquid water rises through a rock column, gas oversaturation would occur, leading to bubble nucleation and growth, volume expansion of the gas-liquid mixture, and finally eruption through the solid conduit. This type of eruption has been referred to as cryovolcanism. Other possible types of gas-driven eruptions include eruptions of sulfurous magmas, as well as nitrogen-, ammonia-, and carbon dioxide–based magmas for outer Solar System satellites (Frankel 1996). Chivas et al. (1987) hypothesized that naturally occurring highly compressed volcanic CO_2 at depth may be a major contributor to phreatic volcanic eruptions and maar formation.

Review Outline

In this review, we discuss experimental simulations of gas-driven eruptions and then focus on lake eruptions, including the dynamics, possible triggering mechanisms, and mitigation of the dangers. We then focus on possible ocean eruptions and dynamics. Other types of eruptions possibly occurring in outer Solar System satellites are not covered. As the title of this review implies, explosive volcanic eruptions powered by

dissolved H_2O and CO_2 in magma, for which a huge literature is already available, are not covered.

Experimental Simulations of Gas-Driven Eruptions

Only part of the eruption process, i.e., the part above the surface, is easily observable. The processes below the surface are critical to understanding how an eruption initiates and proceeds, and how the exit velocity is reached. To understand the processes below the surface, theoretical models, numerical simulations, and experimental simulations using analog systems have been developed. Analog experimental simulations can simulate the full process, including bubble nucleation and growth, upward motion of the bubbly liquid, and heterogeneity of the flow, and can be used to verify theoretical models. Experimental simulations include work on CO_2-water systems, on gum rosin-acetone systems (Phillips et al. 1995), and on hydrovolcanic systems (Zimanowski et al. 1997). Below, the focus is on CO_2-water systems because it is the most relevant to lake and ocean eruptions.

The pioneer of analog experimental simulations of gas-driven eruptions was an aeronautical engineer at the California Institute of Technology, Brad Sturtevant, who unfortunately died at a relatively young age in 2000 (Zhang et al. 2002). Experimental simulations have progressed from simple to more complicated and realistic. In the earlier years, shock wave experiments were carried out by suddenly decompressing a high-pressure gas (Shepherd & Sturtevant 1982, Kieffer & Sturtevant 1984), and the dynamics of the shock wave were investigated. Later experiments used a one-component system that was initially liquid and then was suddenly decompressed into a gas to generate an evaporation wave (Hill & Sturtevant 1990).

In a gas-driven eruption, however, there are at least two components: one is liquid and stays as a liquid, and one is a gas component that initially is dissolved in the liquid but later exsolves to a gas phase. Realizing this, two groups collaborated with Sturtevant and carried out experimental simulations using two-phase (gas-liquid) binary systems. In one experimental approach, water with high dissolved content of CO_2 in a test cell was suddenly decompressed, leading to CO_2 supersaturation, bubble nucleation and growth, volume expansion, and eruption (Zhang et al. 1992, 1997; Mader et al. 1994, 1997; Zhang 1998). In another approach, a K_2CO_3 solution was injected as jets into an HCl solution in a test cell, leading to the formation of high CO_2 concentrations, supersaturation, and eruption (Mader et al. 1994, 1996).

One kind of experimental apparatus is shown in **Figure 2**. It consists of a small glass test cell and a large tank separated by an aluminum diaphragm. The test cell may be either a cylinder with ID $=$ 25 mm and variable lengths (Zhang et al. 1997) or a flask-shaped cell (Mader et al. 1997, Zhang 1998). To examine the effect of viscosity, polymers were added to the water to increase solution viscosity. Prior to an experiment, the test cell housed CO_2-saturated liquid at pressures of several atmospheres. The tank could be evacuated to a desired pressure below one atmosphere. An experiment was initiated as a pneumatically driven knife in the large tank came down to cut the diaphragm. The process was recorded on high-speed film

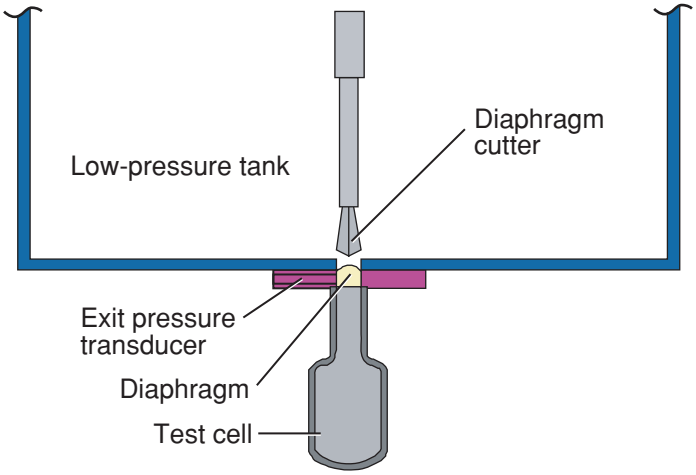

Figure 2

Apparatus for experimental simulation of gas-driven eruptions (from Zhang et al. 1997, Zhang 1998).

(usually 4000 frames per second). The pictures reveal visually and in detail the processes of the gas-driven eruption. Sequences of chosen frames for some simulated eruptions can be seen in Zhang et al. (1997). Two motion pictures can be found by following the Supplemental Material link from the Annual Reviews home page at **http://www.annualreviews.org.**

By analyzing the films frame by frame, bubble nucleation was found to be rapid, with a typical incubation time of a couple of milliseconds. Most bubbles nucleate in the first wave of nucleation, lasting a few milliseconds. Few bubbles form later. The motion of the eruption front in the test cell is characterized by a constant acceleration. Bubbles grow to millimeter size in the order of 10 milliseconds.

Another type of experimental apparatus is used by the Bristol group (Mader et al. 1994, 1996). It consists of a glass test cell (ID = 37 mm) connected to a large reservoir. Inside the test cell there is an injector unit with 96 injection holes that can be shut or open. Prior to an experiment, an HCl solution is fed into the test cell, and a K_2CO_3 solution is fed inside the injector. An experiment is initiated by opening the holes, and 96 turbulent jets of K_2CO_3 solution are injected into HCl solution. The mixing and reaction between HCl and K_2CO_3 generates molecular CO_2, resulting in gas supersaturation and leading to violent eruption. Because of the heterogeneous distribution of K_2CO_3, the resulting flow is also spatially heterogeneous. Frame-by-frame analyses show that bubble nucleation is rapid. The eruption front motion is characterized by an acceleration that increases with time, rather than a constant acceleration as in the first class of experiments.

The above experiments differ from natural eruptions in detail. Compared to explosive volcanic eruptions, driving mechanisms are similar (volume expansion drives up bubbly liquid within a solid conduit), but the material properties are very different. In the experiments, water is a low-viscosity liquid. Even by adding a polymer to increase its viscosity, the viscosity is still many orders of magnitude less than that of hydrous silicic magma. Compared to lake eruptions, material properties are

similar, but the driving mechanisms are different. In the experiments, volume expansion drives the bubbly liquid up the solid test cell, but in lake eruptions, there is no fixed solid conduit, and buoyancy drives up the less-dense bubbly liquid. The experiments are actually most similar to human-controlled degassing of the lakes (see later discussion).

These experiments clearly showed that dissolved CO_2 can drive eruptions, which was a critical step in understanding lake eruptions. Rapid bubble nucleation and growth rates in the experiments may be used to argue that there is quasi-equilibrium between gas phase and liquid phase during lake eruptions, another critical step in modeling the dynamics of lake eruptions. On the other hand, application of the dynamic data from small-scale experiments to large-scale gas-driven eruptions requires consideration of scaling and dynamic similarity. However, no scaling relationships have been established for rapidly degassing bubbly liquids. Hence, models still must be developed to understand the various kinetic and dynamic processes of lake eruptions.

LAKE ERUPTIONS

Local Geology and Background

Lakes Nyos and Monoun lie on the Cameroon Volcanic Line, an intraplate alkaline volcanic chain extending 1600 km from the African continental interior into the oceans to the island of Annobon (Barfod et al. 1999). The lakes are maars (Kling et al. 1987), and Lake Nyos covers an area of approximately 1.5 km^2 and has a maximum depth of ~210 m. Lake Monoun is smaller, with a maximum depth of ~99 m. The region has been volcanically active for many million years, and Mount Cameroon near the center of the chain erupted several times in the past century (Fitton 1987) and as recently as 2000. The region is known by geologists for CO_2-charged, slightly thermal soda springs (Tanyileke et al. 1996), a common feature of volcanic areas, and the CO_2 comes from magma at depth by percolation through the overlying rocks. For example, magmatic CO_2 emission has been documented at Mammoth Mountain of California (Farrar et al. 1995).

When upward-migrating magmatic CO_2 reaches Earth's surface, it dissolves in local groundwater and enters the bottom of a lake. The solubility of CO_2 in water has been studied experimentally and is well-known. It increases with increasing pressure and decreases with increasing temperature. At 25°C, the solubility of CO_2 in water (**Figure 3**; Murray & Riley 1971; Weiss 1974; Wilhelm et al. 1977; Weast 1983) is 0.15 wt% at 0.1 MPa, 1.5 wt% at 1 MPa, 1.6 wt% at 1.1 MPa (pressure at the bottom of Lake Monoun), and 3.1 wt% at 2.1 MPa (pressure at the bottom of Lake Nyos).

Solution of CO_2 increases the density of water (**Figure 4**) and tends to stabilize the CO_2-bearing layer at depth. As CO_2 concentration increases, the water density increases, which promotes a larger density gradient between overlying, CO_2-poor water. Thus, independent of density differences caused by temperature or dissolved salts, a lake can become stably stratified by CO_2 additions alone.

The gas content in Lakes Nyos and Monoun has been monitored since their eruptions (Kling et al. 1994, 2005; Kusakabe et al. 2000). Both lakes contain high

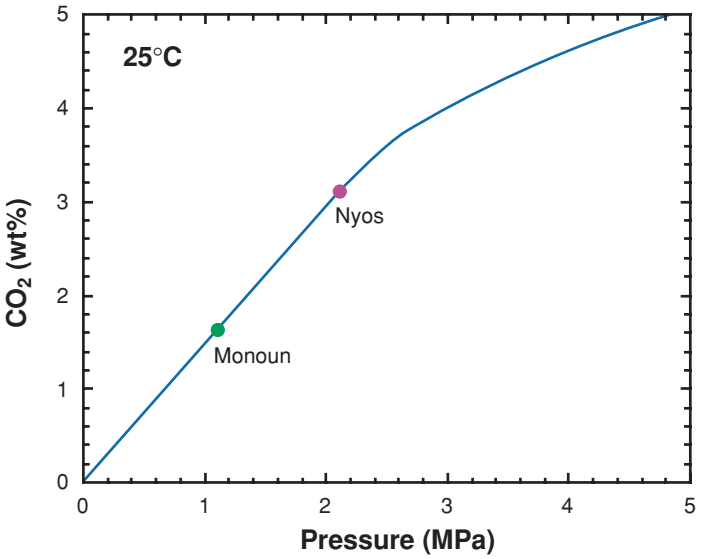

Figure 3

Solubility of CO_2 in water as a function of pressure at 25°C. The bottom water temperature is ~25.2°C at Lake Nyos and ~24.4°C at Lake Monoun. The solubility values in the bottom water of Lakes Nyos (2.1 MPa) and Monoun (1.1 MPa) are indicated. Because of the presence of other gases (mostly CH_4), the concentration of CO_2 at gas saturation is smaller than indicated. Solubility data and model are from Murray & Riley (1971), Weiss (1974), Wilhelm et al. (1977) and Weast (1983).

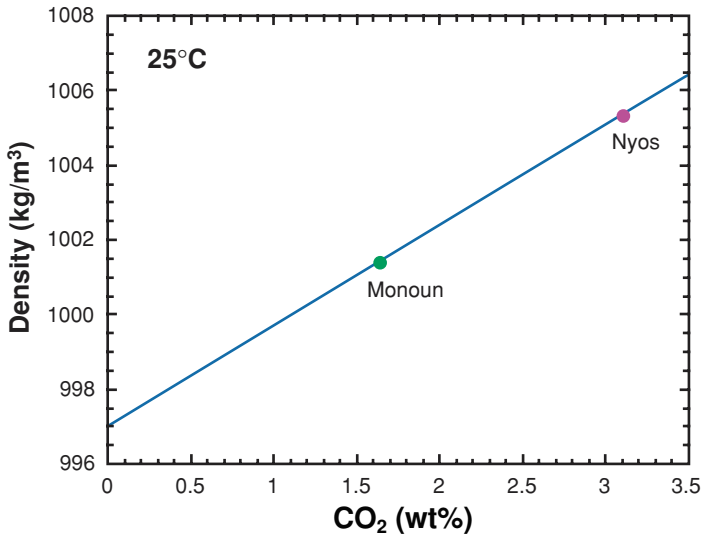

Figure 4

Calculated density of CO_2-bearing water using CO_2 partial molar volume of 32.3×10^{-6} m^3/mol (Weiss 1974). The density values only due to CO_2 of bottom water of Lakes Nyos and Monoun are indicated. The density of bottom water is 1002.1 kg/m^3 in Lake Monoun in 2004, and 1003.7 (at ~10.8 atm P_{CO_2}) in Lake Nyos. The difference between the measured and the calculated density can be attributed to the fact that (*a*) actual lake bottom water is not saturated, (*b*) there are other dissolved gases, and (*c*) there are also dissolved salts.

Figure 5

Sum and partial pressures of dissolved CO_2, CH_4, and N_2 in water of Lake Nyos, January 2003. The hydrostatic line includes atmospheric pressure and represents the saturation level. (Data from W.C. Evans and G. Kling.)

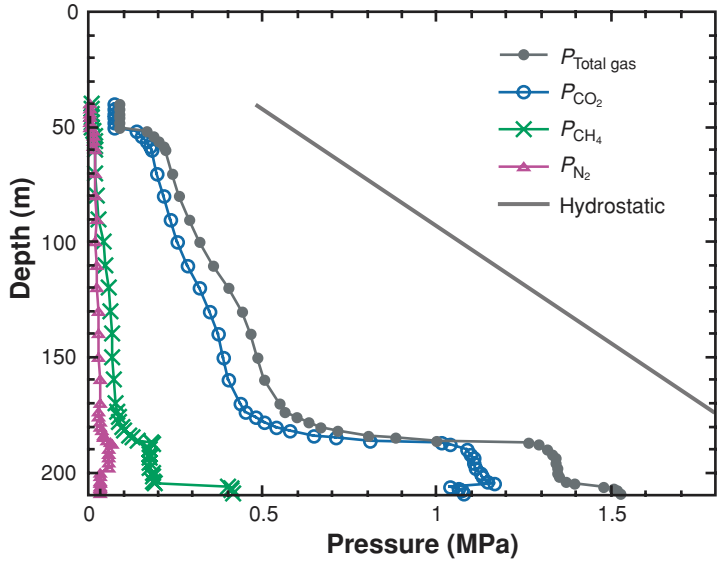

concentrations of CO_2, up to 0.375 mol/kg in Nyos and 0.159 mol/kg in Monoun. In addition to CO_2, there are minor amounts of CH_4 and N_2 (approximately 1.8% and 0.1% of total dissolved gas, respectively), but because CH_4 is so insoluble, it alone contributes up to 27% of the total gas pressure at the lake bottom (**Figure 5**). The dissolved gas pressures increase with depth (**Figure 5**) and have increased over time (Kling et al. 1994, 2005). For example, in Nyos at 206 m depth gas pressures increased from 1.06 MPa in 1990, to 1.29 MPa in 1998, to 1.54 MPa in 2001 before controlled degassing began. A similar trend occurred in Lake Monoun, where the gas pressure at 96 m increased from 0.59 MPa in 1990 to 0.77 MPa in 2003. These trends clearly indicate CO_2 recharge into the lake bottom, and recent estimates indicate an average CO_2 recharge rate of $(1.26 \pm 0.48) \times 10^8$ mol/year into Nyos, and $(8.2 \pm 1.5) \times 10^6$ mol/year into Monoun (Kling et al. 2005). This trajectory of gas increases is alarming, and at present both lakes contain more CO_2 than was likely released during the 1980s disasters—thus, the continued efforts of degassing are imperative.

A stably stratified lake may erupt under at least two scenarios. One is when CO_2 concentrations in bottom water become sufficiently supersaturated, leading to nucleation and growth of bubbles. The bulk density of bubbly water is roughly the density of CO_2 saturated water times (1-*F*) where *F* is the volume fraction of bubbles. For example, Lake Nyos bottom water density at CO_2 saturation would be approximately 1005 kg/m^3. With about 1 vol% of bubbles, the density of the bubbly water would decrease to 995 kg/m^3, lower than bubble-free water at any depth in the lake. At some value of *F* the bottom water would become unstable and the bubbly water would rise buoyantly. As it rises, the surrounding pressure becomes less and bubbles increase in number and expand. The density decreases further and the bubbly water rises with increasing speed. Therefore, the eruption is a strongly positive-feedback process. At

some point, the water film on bubble walls ruptures and the flow fragments into a gas flow carrying water droplets. As the flow exits the lake surface, larger droplets rain down near the eruption vent and finer droplets are carried further away, similar to the mist observed by survivors of the Nyos and Monoun disasters. Because of its high density, the erupting CO_2-water mixture would eventually collapse down to the surface, forming an ambioructic flow.

The second scenario leading to a lake eruption is through perturbation of undersaturated bottom water. The perturbation may be caused by any input of energy that moves deeper, undersaturated water upward in the water column to the point of supersaturation. This energy input may come in many different forms, such as an internal wave, a landslide into lake bottom, density currents of cold water, an earthquake, or volcanic or hydrothermal injections into the bottom of the system (Kling 1987; Kling et al. 1987). The triggering mechanism is important to the specific eruptions, but not to the general understanding of lake eruptions because the trigger may differ from one eruption to another. Furthermore, even without any trigger, eruptions can still happen as long as there is enough oversaturation. Both Zhang (1996) and Woods & Phillips (1999) modeled lake eruption by simply allowing lake water to reach oversaturation.

CO_2 Bubble Growth and Ascent in Lake Water

Many processes are happening at the same time during a lake eruption. Essential component processes in lake eruptions include bubble nucleation and bubble growth because volume expansion owing to gas exsolution leads to buoyancy and ascent of bubbly water. Bubble nucleation in lake water is not quantitatively understood. Because lake water is not free of particles, it is expected that nucleation is heterogeneous and is relatively easy. Nevertheless, quantification of the number density of bubbles (number of bubbles per unit volume of liquid) as a function of time and other parameters (such as degree of oversaturation) has not been carried out. Growth of a single rising bubble can be modeled using a recently developed theory (Kerr 1995, Zhang & Xu 2003, Zhang 2005). The theory is able to calculate the convective growth or dissolution of a rising or falling crystal/droplet/bubble without any free parameters, and has been verified by laboratory experimental data (Zhang & Xu 2003) and in situ experimental data on CO_2 droplet dissolution in ocean water at 800 to 400 m depth (Brewer et al. 2002) modeled by Zhang (2005). The required input parameters include the solubility and diffusivity of the component in water. Calculated bubble growth rate is shown in **Figure 6** (as a function of depth and CO_2 content). At shallow depths, bubble growth rate is often greater than 1 mm/s (depending on the saturation pressure). Even at a depth of 150 m, the growth rate is still 0.05 mm/s for a saturation depth of 208 m, meaning that within 10 s the bubble radius would be 0.5 mm. The high bubble growth rate means that the gas phase and liquid phase may be close to equilibrium. The dynamics of the controlled degassing of Lake Nyos (to be discussed later) also supports the idea that the degassing process is close to equilibrium.

Figure 6

Calculated growth rate at 22°C for a rising bubble as a function of depth (pressure), initial bubble size (a_0), and the dissolved CO_2 content (in terms of CO_2 partial pressure). (*a*) Convective bubble growth rate as a function of depth for two different bubble sizes when the dissolved CO_2 partial pressure is 2.2 MPa. It can be seen that the bubble growth rate only weakly depends on the bubble size. (*b*) Convective bubble growth rate as a function of depth for five different dissolved CO_2 contents (corresponding to partial pressure of 2.2, 1.5, 1.0, 0.5, and 0.2 MPa). Negative growth rate means that the bubble dissolves.

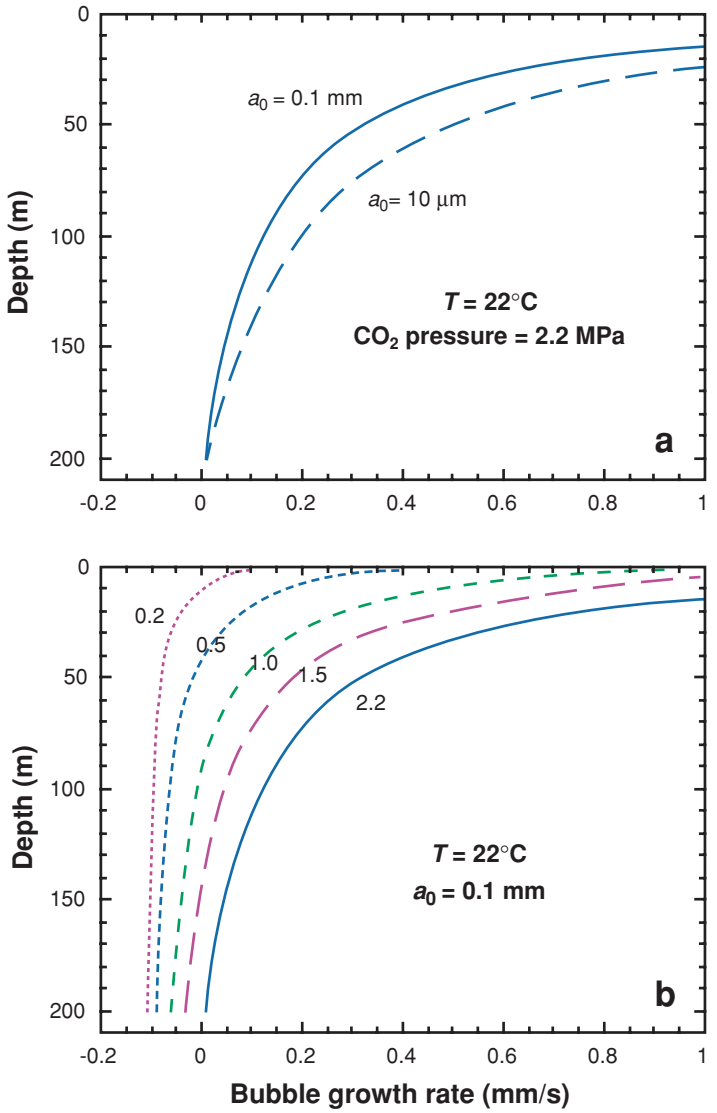

Dynamics of Underwater Bubble Plumes

The dynamics of lake eruptions can be divided into two stages, one is below the lake surface (underwater bubble plume) and one is above the lake surface (eruption column in air). In this section, we discuss the dynamics of underwater bubble plumes. Two semiquantitative models are available in the literature: one is based on the energetics of CO_2 exsolution from water (Zhang 1996) and the other examines whether a small CO_2 flux to the bottom of the lake can be amplified to a large flux similar to that in a lake eruption (Woods & Phillips 1999).

Woods & Phillips (1999) examined the motion of turbulent bubble plumes within lakes containing large quantities of CO_2, such as Lake Nyos. They proposed a model and showed that for a sufficient amount of CO_2 in the lake or a sufficient flux of CO_2 at the base of the lake, a turbulent bubble plume can rise through the lake and erupt at the surface. Owing to the rapid entrainment of ambient water that contains CO_2, the surface flux of CO_2 may be 10^4–10^5 times greater than that at the base of the lake. The return flow in the lake acts to decrease the CO_2 content at all depths of the lake above the plume initiation, and this eventually leads to the termination of the eruption.

A brief summary of the model by Zhang (1996) follows. By ignoring surrounding water entrainment and by treating the two-phase (bubble-water) flow as an effective one-phase flow (the uncertainty introduced by this is small because rising bubble velocity is small), the flow can be described by the Bernoulli equation:

$$\frac{dP}{\rho_{mix}} + g\,dz + u\,du = 0, \tag{1}$$

where P is pressure, ρ_{mix} is the density of the bubble-water mixture, g is acceleration owing to Earth's gravity, z is vertical distance measured from the depth where the eruption starts, and u is the ascent velocity. Because there is no interface between the erupting flow and the ambient water, the relation between P and depth h is simple:

$$P = P_{atm} + \rho_w g h, \tag{2}$$

where P_{atm} is the atmospheric pressure at lake surface, ρ_w is density of water, and h is depth. If initially (i.e., at pressure P_0) there was no gas phase, and assuming equilibrium between the gas phase and liquid phase, the relation between ρ_{mix} and P is

$$\frac{\rho_w}{\rho_{mix}} \approx 1 - \lambda + \lambda\frac{P_0}{P}, \tag{3}$$

where λ is the Ostwald solubility coefficient for CO_2 in water and is roughly 0.87 at 23°C (Wilhelm et al. 1977). Replacing Equation 3 into Equation 1 and integrating leads to

$$\frac{1}{2}u^2 \approx \lambda\frac{P_0}{\rho_w}\left(\ln\frac{P_0}{P} - 1 + \frac{P}{P_0}\right). \tag{4}$$

For example, assuming oversaturation occurred at the bottom of Lake Nyos with $P_0 = 2.14$ MPa, as the flow exits the lake surface ($P = 0.088$ MPa), the velocity obtained using the above equation is $u = 91$ m/s.

If some gas pressure is contributed by CH_4 and air, because their concentration is small (λ is small), their contribution to the eruption velocity is also small. A more accurate account of a two-component gas mixture can be found in Zhang (2000). A rough treatment of such cases is to replace P_0 by the initial CO_2 pressure (or reduce the value of λ) in Equation 6, leading to a lower eruption velocity. Direct measurements indicate that up to 29.5% of the gas pressure in Lake Nyos is due to other gases (**Figure 5**). Assuming oversaturation occurred at lake bottom, the eruption velocity obtained for Lake Nyos using the energy equation is 71 m/s. At this exit velocity, the plume would be able to rise to a height of ~250 m. The eruption column height

Ostwald solubility coefficient, λ: $\lambda = C_{liq}/C_{gas}$, where C_{liq} is the concentration of dissolved gas component in the liquid and C_{gas} is the concentration of the same gas component in the gas phase. The unit of the two concentrations (either mol/m^3 or kg/m^3) must be the same so that λ is dimensionless

is estimated to be from 80 to 120 m for the 1986 Lake Nyos eruption, based on shoreline erosion and the distribution of dead animals (Kling et al. 1987, Sigvaldason 1989), which implies an exit velocity of 48 m/s for the 120 m column. The difference between 71 m/s and 48 m/s may be attributed to the following: (*a*) the velocity given by Equation 4 is the maximum eruption velocity, and the actual velocity may be significantly lower because of entrainment of surrounding water, (*b*) the true eruption column height was greater than the range of heights inferred, (*c*) the initial saturation depth was significantly less than 208 m, or (*d*) a combination of these factors.

In the semiquantitative treatment of the dynamics of lake eruptions by Zhang (1996), the entrainment of surrounding water is ignored. Furthermore, the process is assumed to be reversible (i.e., the gas phase and the liquid phase are always at equilibrium). Bubble growth calculations in the previous section and discussion on controlled degassing in a later section show that the assumption of equilibrium between the gas and liquid phases is not far off. On the other hand, ignoring the entrainment of surrounding water may produce a significant error.

A more realistic treatment is to use a bubble plume model to approximate lake eruptions. Plume models have been developed (e.g., Morton 1956, Milgram 1983, Turner 1986) and applied to volcanic plumes (e.g., Walker et al. 1971; Wilson 1972, 1976; Wilson et al. 1978, 1980; Kieffer 1984; Turner 1986; Woods 1988, 1995; Sparks et al. 1997; Clarke et al. 2002). However, they have not been applied to lake eruptions. Below, the bubble plume model of Milgram (1983) is adapted to lake eruptions by considering the exsolution of CO_2 from water in the plume.

1. Because of turbulence, the velocity field is very complicated. However, at a scale much larger than turbulent cells, the flow has a mean forward (upward) velocity (which differs from local upward or downward velocities), and other mean properties of the flow may be used. For simplicity and also for understanding the important properties, in treating a rising plume only the mean flow is considered. Entrainment of surrounding water affects the dynamics significantly and is treated empirically. The mean flow is treated as upward and described in a cylindrical system in which the upward direction is z.
2. In a horizontal cross-section of the upward flow, the flow velocity of the bubble plume in lake eruptions is assumed to be a Gaussian distribution (Milgram 1983). That is, the flow velocity is greatest at the center and decreases away from the center:

$$u(r, z) = U\mathrm{e}^{-r^2/b^2}, \tag{5}$$

where U is the flow velocity at the centerline of the plume and is a function of z, b (also a function of z) may be viewed as the effective radius of the plume. The vesicularity distribution is also assumed to be Gaussian:

$$\phi(r, z) = \Phi\mathrm{e}^{-r^2/(\beta b)^2}, \tag{6}$$

where Φ is the vesicularity at the centerline and is a function of z, β is a dimensionless number and is not necessarily 1. Experience shows that β is typically 0.80 ± 0.15 (Milgram 1983). The density can be found as

$$\rho = (1 - \phi)\rho_{\mathrm{liq}} + \phi\rho_{\mathrm{gas}}. \tag{7}$$

For lake eruptions, temperature is assumed to be uniform and constant (i.e., ignoring the cooling effect of gas exsolution in the water-gas system because the temperature drop for an adiabatic rise of the two-phase fluid is 3 to 4 K (Zhang 2000).

3. The liquid volume flux and gas volume flux are treated separately. The liquid volume flux (Q_{liq}, in m^3/s) is as follows:

$$Q_{liq} = 2\pi \int_0^\infty (1-\phi) u r \mathrm{d}r = \pi U b^2 \left[1 - \frac{\beta^2 \Phi}{1+\beta^2}\right]. \quad (8)$$

In the above equation, the first equality is definition, and the second equality is obtained by inserting the expressions of u and ϕ and then integrating. The liquid mass flux equals $\rho_{liq} Q_{liq}$. The gas volume flux (Q_{gas}, in m^3/s) is as follows:

$$Q_{gas} = 2\pi \int_0^\infty \phi (u + u_b) r \mathrm{d}r = \pi \Phi \beta^2 b^2 \left[\frac{U}{1+\beta^2} + u_b\right], \quad (9)$$

where u_b is the bubble slip velocity (ascent velocity of bubbles relative to liquid) and depends on bubble size. If the bubble volume is 20 mm^3, $u_b \approx 0.23$ m/s; if bubble volume is 33,000 mm^3 (nonspherical bubble), $u_b \approx 0.45$ m/s (Tsuchiya et al. 1997). Such small relative motion is ignored and the gas and liquid flow velocities are treated to be identical (although the equations below still carry u_b). The gas mass flux equals $\rho_{gas} Q_{gas,}$ where ρ_{gas} is approximately $P/(RT)$. For CO_2 gas, $R = 188.9\ \mathrm{J \cdot kg^{-1} \cdot K^{-1}}$; for CH_4 gas, $R = 518.3\ \mathrm{J \cdot kg^{-1} \cdot K^{-1}}$. The total volume flux is $Q_{liq} + Q_{gas}$. The total mass flux is

$$\rho_{liq} Q_{liq} + \rho_{gas} Q_{gas} = \pi U \rho_{liq} b^2 \left[1 - \frac{\beta^2 \Phi}{1+\beta^2}\right] + \pi \Phi \rho_{gas} \beta^2 b^2 \left[\frac{U}{1+\beta^2} + u_b\right]. \quad (10)$$

4. The momentum flux of the mean flow is

$$M_{mean}(z) = 2\pi \int_0^\infty [\rho_{liq} U^2 (1-\Phi) + \rho_{gas} (U+u_b)^2 \Phi] r \mathrm{d}r. \quad (11)$$

Because there are eddies, the total momentum flux (which includes the turbulent momentum flux) is different. Only the total momentum flux is related to the total buoyancy. The total momentum flux is empirically calculated as

$$M(z) = 2\pi\gamma \int_0^\infty [\rho_{liq} U^2 (1-\Phi) + \rho_{gas} (U+u_b)^2 \Phi] r \mathrm{d}r, \quad (12)$$

where γ is called the momentum amplification factor. In this simple treatment, a limiting value of 1.1 is used and its variation (Milgram 1983) is ignored. Carrying out the integration leads to

$$M(z) = \pi b^2 \gamma U^2 \left\{ \left[\frac{\rho_{liq}}{2} - \frac{\beta^2 \Phi (\rho_{liq} - \rho_{gas})}{1+2\beta^2} + \beta^2 \Phi u_b \rho_{gas} \left[\frac{2U}{1+\beta^2} + u_b\right] \right] \right\}. \quad (13)$$

5. The total buoyancy is:

$$B(z) = 2\pi g \int_0^\infty (\rho_{liq} - \rho_{gas}) \phi r \mathrm{d}r = \pi (\rho_{liq} - \rho_{gas}) \beta^2 b^2 g \Phi. \quad (14)$$

6. Conservation of momentum:

$$dM/dz = B. \tag{15}$$

7. Conservation of liquid. Because entrainment increases the amount of liquid in the plume, the volume flux of liquid increases as a plume rises. The entrainment of surrounding liquid is assumed to be proportional to the centerline flow velocity and the effective perimeter ($2\pi b$) of the plume as follows:

$$\frac{dQ_{liq}}{dt} = 2\pi\varepsilon bU, \tag{16}$$

where ε is the entrainment coefficient. Although a more advanced expression of ε is available (Milgram 1983), a typical value of 0.1 is taken in this study for simplicity.

8. Conservation of gas. Without gas exsolution or dissolution, $P_{gas}Q_{gas}$ would be independent of z. There would be CO_2 exsolution from the initial water parcel that was oversaturated at depth. For the entrained water, it would likely first absorb some CO_2 because it is less saturated, but would then exsolve CO_2 at shallow depths. For simplicity, it is assumed that entrained water does not exsolve or absorb any gas (i.e., assuming the entrained shallow water would affect the upward velocity and mass flux but not participate in the gas-liquid equilibrium). With the assumption, the calculated exit velocity is a minimum because exsolution of gas at shallow depths is ignored. The expression of Q_{gas} is

$$Q_{gas} = Q_{gas}(0)\frac{P_0}{P} + Q_{liq}(0)\lambda\left(\frac{P_0}{P} - 1\right)\Big/\left(1 - \frac{\rho_{gas}}{\rho_{liq}}\right) \tag{17}$$

where $Q_{gas}(0)$ is the initial gas volume flux (when $P = P_0$), $Q_{liq}(0)$ is the initial liquid volume flux, λ is the Ostwald solubility coefficient (0.87 for CO_2 in water at 296 K; Wilhelm et al. 1977), and P_0 is the saturation pressure of the gas in the initial liquid.

Given the above set of equations and approximations, the plume eruption dynamics may be solved numerically. **Figure 7** shows plume centerline velocity calculated for various initial plume radius b_0. As b_0 increases to 10 km, the centerline velocity approaches the maximum velocity obtained by Zhang (1996). Because Lake Nyos surface area is almost 2 km long but less than 1 km wide, and the lake narrows with depth, b_0 may not exceed ~500 m. Based on the localized nature of the eruption, a b_0 of the order 100 m is assumed, which would produce an exit centerline velocity of ~45 m/s. This is likely the minimum exit velocity.

In summary, results from our new model based on the adaptation of the bubble plume model of Milgram (1983) show that CO_2-driven eruptions can be violent, in qualitative agreement with results from the dynamic models of Zhang (1996) and Woods & Phillips (1999). The predicted exit velocity based on the more realistic bubble plume theory is smaller by about a factor of 2 than the prediction in Zhang (1996). True exit velocity may lie in between these two predicted velocities.

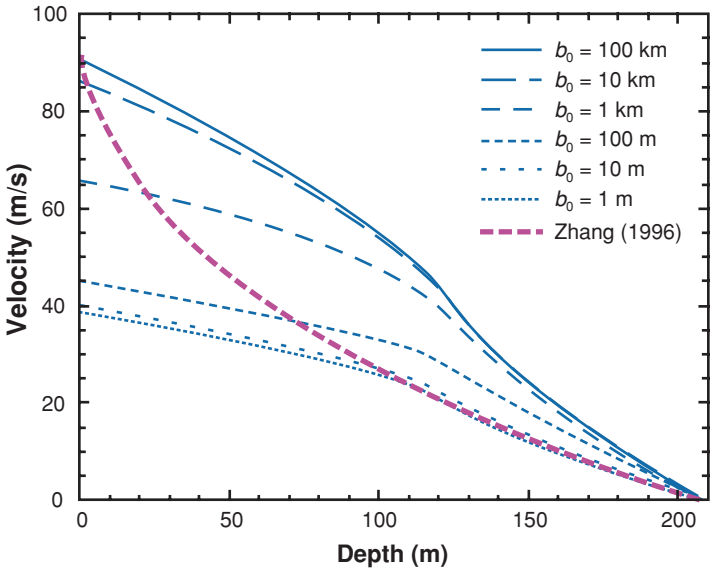

Figure 7

Calculated plume centerline velocity as a function of depth for Lake Nyos assuming CO_2 is saturated in bottom water. The blue curves are for different initial plume radius, and the purple dashed curve is from the semiquantitative model of Zhang (1996).

Dynamics of Eruption Column in Air

After exiting the lake surface, the eruption column might be either a water eruption column carrying bubbles or a CO_2 gas plume carrying water droplets, depending on the extent of bubble fragmentation. To the first order, the relative motion between the two phases may be ignored. Because CO_2 gas is denser than air, the gas plume would reach a maximum height and eventually collapse. Zhang (2004) used a plume model and numerically calculated the maximum eruption height. When the exit plume radius b is greater than 1 m, the eruption height can be estimated by treating the plume as a particle with $H = u^2/(2g)$, where u is the exit velocity. For example, a 45 m/s exit velocity would lead to an average height of 103 m. The center part would rise to a greater maximum height than the rim of the plume owing to larger center velocity.

Dynamics of Degassing Lake Monoun and Lake Nyos

Because the CO_2 content in bottom water of Lakes Nyos and Monoun increased continuously after the two lakes erupted in the 1980s, there is the danger for them to erupt again. Fortunately, with an understanding of the eruption mechanism, scientists and engineers have designed methods to degas the lakes slowly to prevent future eruptions. Halbwachs et al. (2004) reviewed the technical aspects of degassing Lakes Nyos and Monoun, and Kling et al. (2005) presented changes in gas content, lake stability, and predictions for future hazards given various degassing scenarios. The method of degassing is a controlled, small-scale eruption where the CO_2 released dissipates in the atmosphere without forming an ambioructic density flow. The basic design consists of a vertical pipe from the lake bottom to the surface. A small pump, operating close to the top of the pipe, raises the water in the pipe up to a level where it

Figure 8

Eruption jet of Lake Nyos in 2001.

becomes saturated with gas, thus leading to bubble formation and buoyant rise of the two-phase fluid plume with increasing velocity toward the surface. Once the process starts, it sustains itself as long as the gas pressure at the pipe inlet is high enough to provide the exsolution energy to lift water from the level of pump lift.

The feasibility of degassing by this method was demonstrated for Lake Monoun in 1992 and for Lake Nyos in 1995, and operational degassing pipes were installed in Lake Nyos in 2001 and in Lake Monoun in 2003 (Halbwachs et al. 2004, Kling et al. 2005). The eruption jet for Lake Nyos degassing is shown in **Figure 8**, and the full strength eruption jet is about 50 m high. The eruption column height of 50 m for

pipe degassing is much smaller than the inferred eruption column height during the 1986 Lake Nyos eruption.

The dynamics of pipe degassing are different from the dynamics of lake eruptions because the introduction of pipes provides a fixed eruption conduit, resulting in the dynamics of pipe degassing being similar to those of an explosive volcanic eruption. First, with a fixed conduit, there is no entrainment of surrounding water. Second, the speed of a compressible fluid flow constrained by a constant-radius conduit cannot exceed the sound speed of the fluid (i.e., gas-liquid mixture), and is often the same as the sound speed when the initial gas content is high (meaning that there is enough energy to produce a much higher speed). For example, explosive volcanic eruption velocity is often regarded to be the same as the sound speed of a gas-magma mixture (e.g., Woods 1995). The general equation for estimating the sound speed of a two-phase mixture is as follows (Mastin 1995):

$$u_s = \sqrt{\frac{dP}{d\rho_{mix}}} = \sqrt{\frac{B_{liq} B_{gas}}{\rho_{mix}[(1-\phi)B_{gas} + \phi B_{liq}]}}, \quad (18)$$

where u_s is the sound speed, B is the bulk modulus (or 1 over the compressibility), and ϕ is the volume fraction of the gas phase (vesicularity). For an ideal gas, $B_{gas} = P_{gas}$. For water, B_{liq} is very large (about 2.2 GPa). With $\phi B_{liq} \gg (1-\phi)B_{gas}$, the above equation can be simplified to

$$u_s \approx \sqrt{\frac{P}{\phi(1-\phi)\rho_{liq}}}. \quad (19)$$

For Lake Nyos degassing with $P_0 = 1.24$ MPa (this is the maximum P_{CO_2} measured ~1 month before the degassing operation at the depth of the pipe inlet), $P = 0.088$ MPa (for Lake Nyos surface), and $\lambda = 0.87$, if equilibrium were reached, then using Equation 3, it is derived that $\rho_{mix} = 0.08\rho_{liq}$, which is the minimum density that can be reached. The calculated sound speed using Equation 19 is 35 m/s, which would be the maximum eruption velocity as the flow exits the pipe. With this initial velocity, the eruption column height would be about $u^2/(2g) = 62$ m.

Halbwachs et al. (2004) reported the observed density of the discharge fluid, the discharge rate, and the eruption height. The observed density of the discharge fluid is about $0.1\rho_{liq}$, which is slightly above the minimum density as expected. Hence the assumption of perfect equilibrium is not far off. From the density of the mixture, it can be found that $\phi \approx 0.9$ and the respective sound speed is 31 m/s. At this speed, the column would rise to a height of ~50 m, consistent with observations. (This velocity would imply a water discharge rate of 0.05 m^3/s; the reported water discharge rate of 0.07 m^3/s seems to be slightly too high.)

In summary, the theoretical analysis of pipe degassing dynamics is for the most part consistent with observed eruption data. The controlled pipe degassing process is not far from equilibrium, and the exit eruption velocity does not differ much from the sound speed.

Other Lakes

One may wonder whether a specific lake may erupt in the future. Five conditions must be met for a violent lake eruption to occur. One is that the lake must be deep; for example, a lake 10 m deep would have no ability to store large amounts of gas and thus no potential to erupt violently, and this potential would increase as lake depth increases. The second condition is a continuous source of gas supplied to the bottom of the lake so that bottom water gradually becomes saturated. The third is that the gas supplied into the bottom water must have a high solubility because the erupting energy is proportional to the solubility coefficient (solubility at a specific pressure) according to Equation 4. The greater the solubility coefficient, the more violent the eruption can be. For example, the solubility coefficient of CO_2 in water is 45 times that of air and 26 times that of CH_4. Therefore, energy obtained from the exsolution of air from water (or methane from water) would be less than that obtained from the exsolution of CO_2 from water by the appropriate factor. The fourth is that the gas must accumulate in the bottom waters. That is, the surface and bottom water of the lake must not mix for periods long enough for gas to accumulate to dangerous amounts. Unless stabilized by high salt content in bottom waters, most lakes mix every year owing to the sinking of surface water as the surface temperature cools in autumn or winter, and thus the lake would regularly release any inputs of gas to the atmosphere. The fifth is that the dissolution of gas must increase the density of water. Otherwise, the gas dissolution would lead to decreased density and buoyant rise of the water causing mixing and the loss of gas from the lake. These conditions mean that gas-driven lake eruptions are most likely to occur in deep equatorial lakes near volcanic zones. For example, bottom water from deep Crater Lake and Lake Tahoe was collected some years ago, and no high concentrations of CO_2 were found.

The third lake known to contain high concentrations of gas is Lake Kivu, Africa, which covers an area of 2700 km^2 with an average depth of 220 m and a maximum depth of 475 m. As reported in Schmid et al. (2002/2003), in 1975 it contained about 250 km^3 CO_2 and 55 km^3 CH_4 at standard temperature (273.15 K) and pressure (1 atm). Near the maximum depth, where the hydrostatic pressure is about 4.7 MPa, CH_4 partial pressure was about 1.4 MPa and CO_2 partial pressure was about 0.4 MPa (Schmid et al. 2002/2003). It is unclear how much the gas contents have increased since 1975. Because it is still far from saturation, small perturbations would not be able to trigger a lake eruption. Furthermore, even though the total gas pressure is about the same as that of Lake Nyos in 2001, the total gas concentration (in mol/L) in the bottom water of Lake Kivu is only about one fourth of that of Lake Nyos because most of the gas pressure is due to CH_4. Hence it is expected that even if an eruption were triggered, it may not be as violent as the eruption of Lake Nyos. Using a numerical scheme (Zhang 2000) to integrate the Bernoulli equation as the two gas components CO_2 and CH_4 exsolve from water, the maximum eruption velocity would be only 23 m/s. Because of shallow water entrainment, the actual eruption velocity would be less than 23 m/s. Although the eruption velocity may be lower than in Lake Nyos, there is a tremendous amount of gas contained in Lake Kivu and there are

several million people living close to the lake in the surrounding basin that could be affected by a gas release.

CARBON SEQUESTRATION BY INJECTING LIQUID CO_2 INTO OCEANS

Anthropogenic activities have significantly increased the atmospheric content of CO_2, a main greenhouse gas. To mitigate this increase, one idea is to sequester CO_2 by injecting liquid CO_2 into oceans. At less than 2000 mbsl (meters below sea level), CO_2 liquid is less dense than seawater and would rise. Because seawater is undersaturated with respect to liquid CO_2, the droplets also dissolve as they rise. Brewer et al. (2002) carried out in situ experiments, measuring the rise and dissolution of two CO_2 droplets with initial radius of 4.5 mm as they rise from about 800 mbsl to about 400 mbsl. **Figure 9** shows that a recently developed theory (Zhang & Xu 2003) is able to predict the dissolution of CO_2 droplets without any free parameters (Zhang 2005). Therefore, the dissolution trajectory of CO_2 droplets can be calculated at any depth and temperature in the oceans. Calculation shows that a CO_2 droplet with a radius of 5 mm is able to survive a 400-m seawater column (depending slightly on temperature and initial depth). Larger droplets can survive longer travel through a water column.

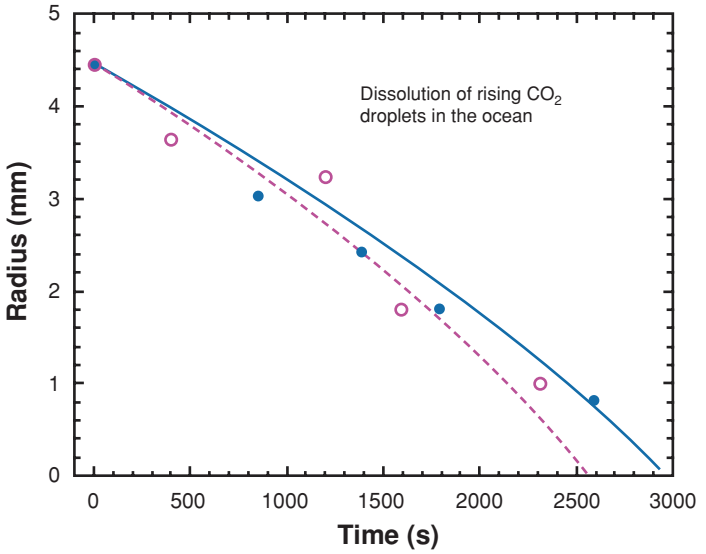

Figure 9

Comparison of experimental data (Brewer et al. 2002) for the dissolution of two rising CO_2 liquid droplets, droplet 1 starting at 804.5 m depth (*blue solid circles*), and droplet 2 starting at 649.1 m depth (*purple open circles*), with calculated curves (*blue solid curve* for droplet 1 and *purple dashed curve* for droplet 2). Directly measured temperature-depth relation is used in calculating the density and solubility of CO_2 droplets. The effect of salts on the calculation has been accounted for. From Zhang (2005) with correction of one data point.

If CO_2 droplets rise to a shallow level where CO_2 gas is more stable than liquid (about 400 mbsl, depending on seawater temperature), CO_2 liquid converts to gaseous CO_2. If the amount of gas is small and not concentrated, bubbles would rise and dissolve in seawater. If a large amount of concentrated CO_2 gas is formed at this depth, the gas-bearing water might rise as a CO_2 bubble plume to reach the atmosphere, and thus defeat the purpose of carbon sequestration. Furthermore, the CO_2 bubble plume might erupt violently if the amount of CO_2 is high, similar to a lake eruption reviewed above. In designing injection schemes, it is important to avoid such consequences. One method would be to inject CO_2 to a depth of 3000 mbsl. Then CO_2 liquid would be denser than seawater, and would sink and dissolve. The environmental consequences of dissolved CO_2 must also be evaluated, but it is outside the scope of this review.

POSSIBLE METHANE-DRIVEN OCEAN ERUPTIONS AND DYNAMICS

Methane Hydrate and Gas in Marine Sediment and Phase Relations

The properties of methane hydrate have been reviewed by Buffet (2000). CH_4 in marine sediment may be in the forms of methane hydrate, free methane gas, and dissolved CH_4 in pore water. The amount of CH_4 in hydrate is uncertain but huge. Kvenvolden (1988) estimated that 2×10^{16} kg of carbon are in the form of methane hydrate, indicating that methane hydrate and gas in marine sediment is the largest hydrocarbon reservoir on Earth. The huge amount of CH_4 in marine sediment, if released to the atmosphere, would cause major and rapid global warming. It is also hypothesized that rapid release of CH_4 could lead to oceanic eruptions and mass extinctions (Ryskin 2003, Zhang 2003). Because $\delta^{13}C$ in various forms of CH_4 is much lower than $\delta^{13}C$ in carbonate in seawater and CO_2 in the atmosphere, the release of a large amount of methane can be and has been inferred from negative $\delta^{13}C$ excursions in sedimentary records (e.g., Dickens et al. 1995, Kennett et al. 2002).

To understand the complicated kinetic and dynamic behavior of CH_4 in the ocean environment, it is critical to first understand the phase equilibrium in the CH_4-H_2O system. A typical CH_4-H_2O phase diagram in an ocean environment along a hydrotherm and geotherm is shown in **Figure 10**. In very shallow seawater, methane hydrate is not stable owing to low ambient pressure. Starting from about 500 mbsl to about 450 m below the sea floor (both values depending on the local temperature), methane hydrate is stable as long as CH_4 concentration is high. At depths greater than 450 m below the sea floor, methane hydrate is not stable owing to high temperature, and some CH_4 would be present in the gas phase (as bubbles). The presence of a gas-methane boundary in marine sediment means that if the geotherm is suddenly elevated, a large amount of methane hydrate may rapidly convert to methane gas, leading to increased pressure and gas bursts. Such gas bursts may result in mud volcanoes (e.g., Hedberg 1974, Lance et al. 1998, Aloisi et al. 2000,

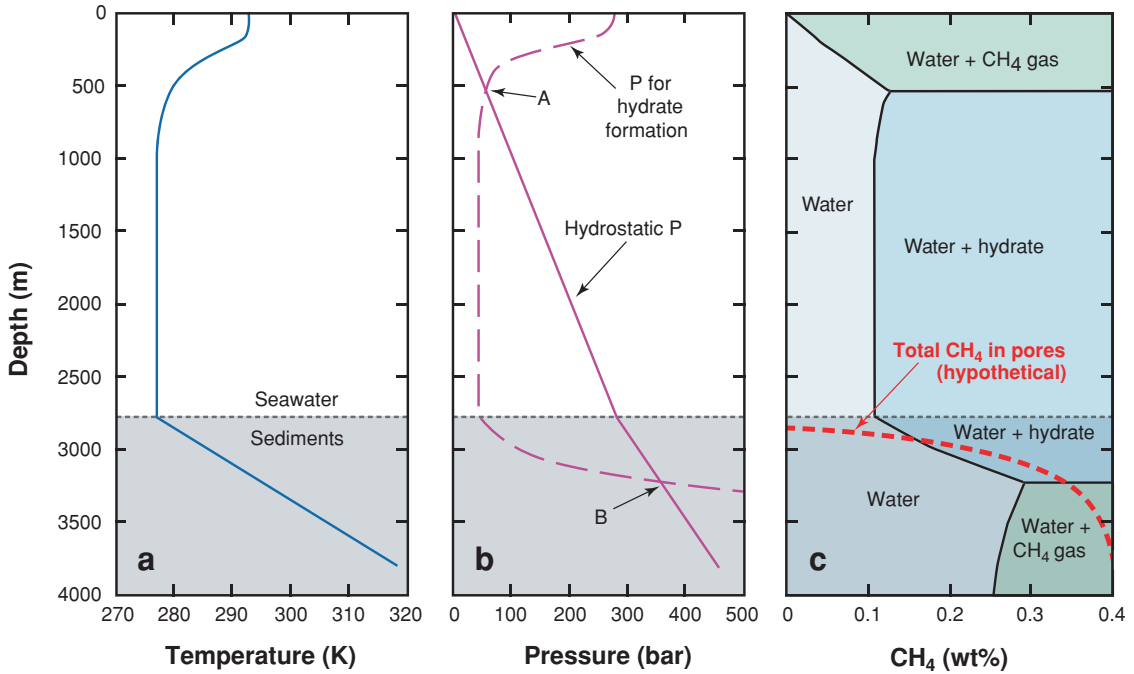

Figure 10

A typical phase diagram of the CH_4-H_2O system in the oceanic environment for water depth >600 m. (*a*) Temperature profile (roughly corresponding to the case of Blake Ridge east of Carolina). The dashed horizontal line in (*a*), (*b*), and (*c*) marks the sea floor. (*b*) Hydrostatic pressure (*solid curve*) and hydrate-stability pressure (*dashed curve*) as a function of depth. (*c*) Calculated phase diagram for the temperature and hydrostatic pressure given in (*a*) and (*b*). Solid curves mark phase boundaries. The red dashed curve marks hypothetical total CH_4 concentration (in the form of dissolved CH_4, CH_4 gas, and CH_4 hydrate) in pore spaces. (From Zhang 2003.)

Milkov 2000, Kopf et al. 2001). According to the phase diagram for CH_4-H_2O system (**Figure 10**), methane gas would convert to methane hydrate in the sediment column or upon reaching the sea floor (>530 mbsl). In the sediment column, if pore water is already saturated with CH_4, methane gas bubbles would first react with water to form a hydrate shell, and the shell thickness would gradually grow to convert the entire bubble into hydrate. In the water column, or when pore water is undersaturated with CH_4, methane bubbles would also first react with water to form a hydrate shell. The hydrate shell would dissolve on the outer surface and grow on the inner surface, so that there would be a delicate dynamic balance that leads to a steady-state shell thickness. This thickness depends on the dissolution regime (such as diffusive dissolution versus convective dissolution of a rising shelled bubble), and the theory for estimating such thickness is being developed (Gabitto & Tsouris 2005).

Kinetics and Dynamics of Methane Hydrate Dissolution and Dissociation

Methane hydrate and methane bubbles may be released to the ocean water column owing to either gas bursts, mega-landslides, or other processes. Once methane hydrate crystals and methane gas bubbles are released to the water column, because they are less dense than seawater, they would rise and dissolve in water. As shown by the CH_4-H_2O phase diagram (**Figure 10**), the behavior depends on the sea floor depth. If the sea floor depth is less than 530 mbsl, then only methane gas is stable in the water column and the sediment column (**Figure 11**), and released methane gas would rise as streams of bubbles or as a bubble plume if both the number density and the total number of bubbles are large. The dynamics of such a bubble plume may be modeled in a similar fashion as CO_2 bubble plumes in lake eruptions (see below).

If the sea floor depth is greater than 530 mbsl, then on the sea floor and its adjacent water and sediment column, methane hydrate is stable. Released methane hydrate would stay as hydrate and would rise and dissolve in the water column. Released methane gas bubbles would react with seawater to form a hydrate shell and would

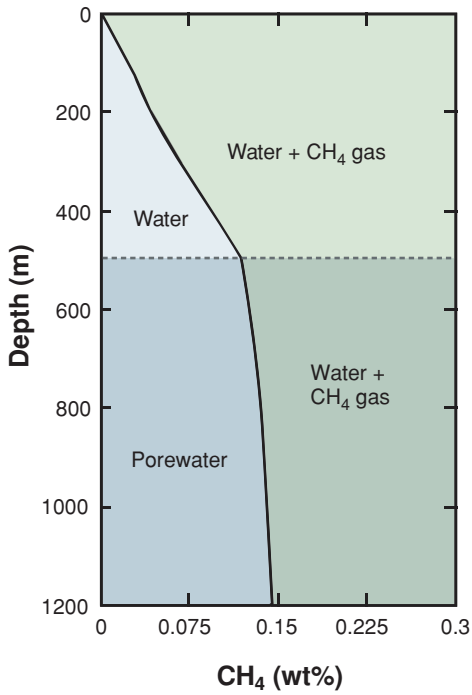

Figure 11

A phase diagram of the CH_4-H_2O system in the oceanic environment for a water depth of 500 m. The dashed horizontal line marks the sea floor. Below the sea floor, the solubility does not increase with depth as rapidly as in seawater owing to temperature increase with depth in sediment.

rise and dissolve as shelled gas bubbles. The formation of a hydrate shell reduces the stability of CH_4 in water and the dissolution rate. The water parcel containing hydrate and shelled bubbles may or may not rise as a plume (depending on the number density and total amount). In any case, hydrate crystals and shelled bubbles would rise and dissolve. One question is whether these CH_4 forms are able to survive the water column and reach a shallow level (530 mbsl) where they would convert into gas and turn into a gas bubble plume to vent into the atmosphere. Zhang & Xu (2003) examined this question and showed that a hydrate crystal with a diameter of 10 mm is able to rise about 2000 m relative to water. Once the hydrate reaches the dissociation boundary (dashed horizontal line in **Figure 10** at 530 mbsl) it dissociates rapidly. Shells on gas bubbles would also dissociate rapidly. A hydrate crystal with a diameter of 10 mm would dissociate completely in a 47 m water column. To survive a water column of 530 m, the hydrate sphere must have an initial diameter of about 0.1 m (depending on the local temperature-depth profile). Therefore, if there is a large amount of methane hydrate, and methane gas is released to the seawater column, under the right conditions it is possible that a large and concentrated bubbly plume could form at about 500 m water depth and lead to a surface eruption.

Bubble Plumes

The dynamics of methane bubble plumes in seawater have not been investigated experimentally or theoretically in detail. The Discovery Channel ("Dive to Bermuda Triangle," 4 April 2004) showed some interesting experiments by Guy Meadows and his coworkers at the University of Michigan to investigate the rise of huge bubbles, especially on the ability of bubble plumes to sink boats. Zhang (2003) developed a semiquantitative model to estimate the exit velocity of CH_4-water plumes, similar to his lake eruption model (Zhang 1996). Below, our adaptation of the plume model of Milgram (1983) for lake eruptions is applied to methane bubble plume eruptions. Because the CH_4 concentration in ambient water at the depth of hydrate dissociation is difficult to estimate, it is assumed that no CH_4 would exsolve from water and no CH_4 would be absorbed by water. The initial depth is assumed to be 500 m, and two values for the initial amount of CH_4 gas from dissociation are examined. The centerline velocity of a methane bubble plume increases with the initial amount of CH_4 gas in the gas phase and the initial plume radius. For an initial plume radius of 10 km, the exit centerline velocity may reach 130 m/s for 1 wt% of the initial fraction of the gas phase (**Figure 12**). If the initial fraction of the gas phase is 0.1 wt%, the exit centerline velocity would be 62 m/s. Hence a concentrated and large CH_4 gas pocket is able to power a violent ocean eruption, although such eruptions have not been observed. Recognizing that gas-powered ocean eruptions may occur would help us understand this phenomenon in the future should it occur, avoiding confusion that occurred when lake eruptions were first discovered.

Because CH_4 gas is less dense than air, after exiting the ocean surface the gas plume would rise high into the atmosphere and gradually dissipate, which differs from the formation of a ground-hugging CO_2 density flow after a lake eruption. In addition, if the plume has sufficiently high CH_4 concentrations it could ignite. Finally, if a

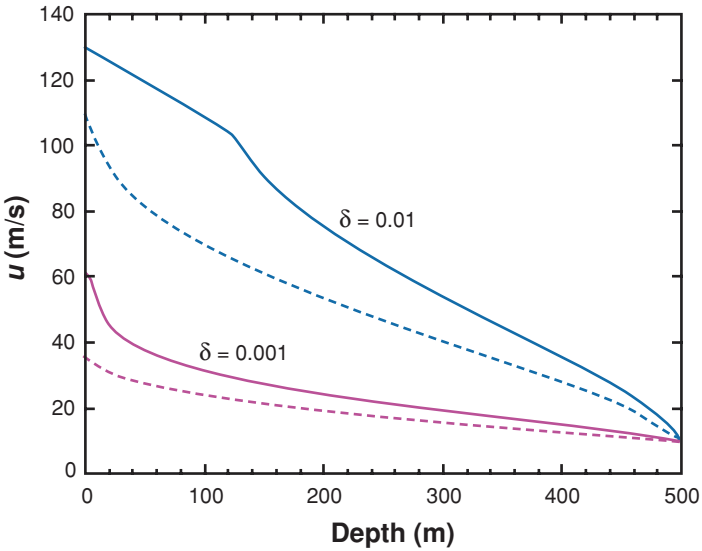

Figure 12

Calculated eruption velocity for a CH_4 bubble plume ascending from a depth of 500 mbsl. The symbol δ is the initial mass fraction of the gas phase. The blue curves are for $\delta = 0.01$, and the purple curves are for $\delta = 0.001$. The solid curves are calculated centerline velocity using the bubble plume model described in the text. The dashed curves are calculated using the semiquantitative theory of Zhang (2003). The initial velocity is assumed to be 10 m/s (varying the initial velocity only changes the exit velocity slightly), and the initial plume radius b is taken to be 10 km (the exit plume radius b is 3.3 km for $\delta = 0.01$ and 5.2 km for $\delta = 0.001$).

CH_4 bubble plume in the ocean encounters an ocean vessel, or a rising plume in the atmosphere encounters an airplane, it would be hazardous, although the exact effects are poorly understood.

SUMMARY

The dynamics of gas-driven lake and ocean eruptions depends on the concentration of the gases when eruption is initiated, the solubility constants, and the conduit radius. The dynamics of underwater lake eruption plumes have been approximated by the Bernoulli equation (Zhang 1996), assuming that there is rough equilibrium between the gas phase and liquid phase and ignoring surrounding water entrainment. Bubble growth calculations and controlled degassing experiments show that the equilibrium assumption is not far off. In this review, to account for the effect of shallow water entrainment, the bubble plume theory of Milgram (1983) is adapted to the specific cases of lake eruptions and possible ocean eruptions. Results from the plume model show that the exit eruption velocity depends on the plume radius. Only for very large radius (of the order 10 km or more) would the exit velocity approach that calculated from the simple Bernoulli equation. For a lake eruption "conduit" radius of 0.1 km,

the centerline exit velocity is only about half of the value predicted using the Bernoulli equation (Zhang 1996). Because of the simplifications in the models, the centerline exit velocity is likely between the calculated plume velocity and Bernoulli velocity. For controlled pipe degassing of the lakes, the exit velocity is roughly the sound speed of the gas-liquid mixture.

The initial discovery of lake eruptions led to puzzlement, surprise, and vigorous debates. Twenty years after the discovery of lake eruptions, scientists have gained a fundamental understanding of the mechanism and dynamics of such processes. With such understanding, the killer lakes are being degassed to reduce the danger of future eruptions. If successful, this will be one of the most triumphant examples of hazard mitigation. The discovery of lake eruptions also helped scientists to realize the varieties of gas-driven eruptions. Such realization leads to the investigation of various other types of hypothetical gas-driven eruption processes, so that humankind will be better prepared for such events.

FUTURE ISSUES

1. Bubble nucleation and growth play fundamental roles in gas-driven eruptions. In bubble growth, large bubbles have complicated shapes and wobble in water, which makes it difficult to calculate the growth rate accurately. Hence, more work using combined experimental and theoretical approaches is necessary to understand the growth of large rising bubbles. In bubble nucleation, there is currently no way to predict bubble nucleation rates in lake water or seawater. Hence, it is impossible to estimate bubble number density during an eruption, which means that the assumption of gas-liquid equilibrium must be used in constructing dynamic models. If nucleation rate can be quantified in the future, then it will be possible to construct more accurate models that incorporate the kinetics of gas exsolution and dynamics of shallow water entrainment in treating bubble plume eruptions.
2. For the mitigation of lake eruption hazards, it is essential to continue surveys and monitoring of equatorial lakes in volcanic regions. Additional effort should be made to degas Lakes Nyos and Monoun more quickly to reduce the window of danger from currently high gas concentrations. It is also important to closely monitor Lake Kivu because it has the potential to produce a much more devastating, in terms of human life, lake eruption.
3. On ocean eruptions, only preliminary work has been done. In the future this research will be dependent on mapping of various methane hydrate regions and other basic research on methane hydrate dynamics. One direction that is directly related to ocean eruptions is to understand the mechanisms of methane hydrate release to the water column from sediment through mud eruptions or other means.

4. Understanding environmental consequences of carbon sequestration in oceans will determine whether this technique is viable. Additionally, more sophisticated models combining the droplet dissolution model with large-scale convection patterns should be developed.

ACKNOWLEDGMENTS

This manuscript was largely written during the authors' sabbatical leave from the University of Michigan. The work is partially supported by Peking University (985 Program by the Chinese Ministry of Education), the US NSF (EAR-0125506, EAR-0228752, EAR-0537598, DEB-0423385), and the US AID (OFDA-AOTA-00–99-00,223–00). Acknowledgment is also made to the donors of the American Chemical Society Petroleum Research Fund for partial support of this research. We thank Eric Essene and an anonymous reviewer for reviewing this paper. YZ thanks Gaston Kayser and Kevin Burke for discussion, and Yong Chen and Xiaodong Song for the beer trick.

LITERATURE CITED

Aloisi G, Pierre C, Rouchy JM, Foucher JP, Woodside J. 2000. Methane-related authigenic carbonates of eastern Mediterranean Sea mud volcanoes and their possible relation to gas hydrate destabilisation. *Earth Planet. Sci. Lett.* 184:321–38

Barfod DN, Ballentine CJ, Halliday AN, Fitton JG. 1999. Noble gases in the Cameroon line and the He, Ne, and Ar isotopic compositions of high μ (HIMU) mantle. *J. Geophys. Res.* 104:29509–27

Brewer PG, Peltzer ET, Friedrich G, Rehder G. 2002. Experimental determination of the fate of rising CO_2 droplets in seawater. *Environ. Sci. Technol.* 36:5441–46

Buffett BA. 2000. Clathrate hydrates. *Annu. Rev. Earth Planet. Sci.* 28:477–507

Bugge T, Befring S, Belderson RH, Eidvin T, Jansen E, et al. 1987. A giant three-stage submarine slide off Norway. *Geo-Marine Lett.* 7:191–98

Chivas AR, Barnes I, Evans WC, Lupton JE, Stone JO. 1987. Liquid carbon dioxide of magmatic origin and its role in volcanic eruptions. *Nature* 326:587–89

Clarke AB, Voigt B, Neri A, Macedonio G. 2002. Transient dynamics of vulcanian explosions and column collapse. *Nature* 415:897–901

Cotel AJ. 1999. A trigger mechanism for the Lake Nyos disaster. *J. Volcanol. Geotherm. Res.* 88:343–47

Crawford GD, Stevenson DJ. 1988. Gas-driven water volcanism and the resurfacing of Europa. *Icarus* 73:66–79

Dickens GR, O'Neil JR, Rea DK, Owen RM. 1995. Dissociation of oceanic methane hydrate as a cause of the carbon isotope excursion at the end of Paleocene. *Paleoceanography* 10:965–71

Evans WC, Kling GW, Tuttle ML, Tanyileke G, White LD. 1993. Gas buildup in Lake Nyos: the recharge process and its consequences. *Appl. Geochem.* 8:207–21
Evans WC, White LD, Tuttle ML, Kling GW, Tanyileke G, Michel RL. 1994. Six years of change at Lake Nyos, Cameroon, yield clues to the past and cautions for the future. *Geochem. J.* 28:139–62
Farrar CD, Sorey ML, Evans WC, Howle JF, Kerr BD, et al. 1995. Forest-killing diffuse CO_2 emission at Mammoth Mountain as a sign of magmatic unrest. *Nature* 376:675–78
Fitton JG. 1987. The Cameroon Line, West Africa: a comparison between oceanic and continental alkaline volcanism. In *Alkaline Igneous Rocks*, ed. JG Fitton, BGJ Upton, pp. 273–91. Boston: Blackwell Sci. Publ.
Frankel C. 1996. *Volcanoes of the Solar System*. Cambridge, UK: Cambridge Univ. Press. 232 pp.
Freeth SJ. 1990. The anecdotal evidence, did it help or hinder investigation of the Lake Nyos gas disaster? *J. Volcanol. Geotherm. Res.* 42:373–80
Freeth SJ, Kay RLF. 1987. The Lake Nyos gas disaster. *Nature* 325:104–5
Freeth SJ, Kling GW, Kusakabe M, Maley J, Tchoua FM, Tietze K. 1990. Conclusions from Lake Nyos disaster. *Nature* 348:201
Gabitto J, Tsouris C. 2006. Dissolution mechanisms of CO_2 hydrate droplets in deep seawaters. *Ener. Conv. Manag.* 47:494–508
Giggenbach WF. 1990. Water and gas chemistry of Lake Nyos and its bearing on the eruptive process. *J. Volcanol. Geotherm. Res.* 42:337–62
Halbwachs M, Sabroux JC, Grangeon J, Kayser G, Tochon-Danguy JC, et al. 2004. Degassing the "killer lakes" Nyos and Monoun, Cameroon. *Eos* 85:281–88
Hedberg HD. 1974. Relations of methane generation to undercompacted shale, shale diapirs, and mud volcanoes. *Am. Assoc. Pet. Geol. Bull.* 58:661–73
Hill LG, Sturtevant B. 1990. *An Experimental study of evaporation waves in a superheated liquid*. Presented at Adiabatic Waves in Liquid-Vapor Systems, IUTAM Symp., 1989, Gottingen, Germany
Kennett JP, Canariato KG, Hendy IL, Behl RJ. 2002. *Methane Hydrate in Quaternary Climate Change*. Washington, DC: Am. Geophys. Union. 224 pp.
Kerr RC. 1995. Convective crystal dissolution. *Contrib. Mineral. Petrol.* 121:237–46
Kieffer SW. 1984. Factors governing the structure of volcanic jets. In *Explosive Volcanism: Inception, Evolution, and Hazards*, pp. 143–57. Washington, DC: Natl. Acad.
Kieffer SW, Sturtevant B. 1984. Laboratory studies of volcanic jets. *J. Geophys. Res.* 103:8253–68
Kling GW. 1987. Seasonal mixing and catastrophic degassing in tropical lakes, Cameroon, West Africa. *Science* 237:1022–24
Kling GW, Clark MA, Compton HR, Devine JD, Evans WC, et al. 1987. The 1986 Lake Nyos gas disaster in Cameroon, West Africa. *Science* 236:169–75
Kling GW, Evans WC, Tuttle ML. 1991. A comparative view of Lakes Nyos and Monoun, Cameroon. *Vereinigung ver. Internat. Limnol.* 24:1102–5
Kling GW, Evans WC, Tuttle ML, Tanyileke G. 1994. Degassing of Lake Nyos. *Nature* 368:405–6

Kling GW, Tuttle ML, Evans WC. 1989. The evolution of thermal structure and water chemistry in Lake Nyos. *J. Volcanol. Geotherm. Res.* 39:151–65

Kling GW, Evans WC, Tanyileke G, Kusakabe M, Ohba T, et al. 2005. Degassing Lakes Nyos and Monoun: defusing certain disaster. *Proc. Natl. Acad. Sci. USA* 102:14185–90

Kopf A, Klaeschen D, Mascle J. 2001. Extreme efficiency of mud volcanism in dewatering accretionary prisms. *Earth Planet. Sci. Lett.* 189:295–313

Kusakabe M, Tanyileke G, McCord S, Schladow G. 2000. Recent pH and CO_2 profiles at Lakes Nyos and Monoun, Cameroon: implications for the degassing strategy and its numerical simulation. *J. Volcanol. Geotherm. Res.* 97:241–60

Kvenvolden KA. 1988. Methane hydrate—a major reservoir of carbon in the shallow geosphere? *Chem. Geol.* 71:41–51

Kvenvolden KA. 1998. A primer on the geological occurrence of gas hydrate. In *Gas Hydrate: Relevance to World Margin Stability and Climatic Change*, ed. JP Henriet, J Mienert, pp. 9–30. London: Geol. Soc.

Lance S, Henry P, Pichon XL, Lallemant S, Chamley H, et al. 1998. Submersible study of mud volcanoes seaward of the Barbados accretionary wedge: sedimentology, structure and rheology. *Mar. Geol.* 145:255–92

Mader HM, Brodsky EE, Howard D, Sturtevant B. 1997. Laboratory simulations of sustained volcanic eruptions. *Nature* 388:462–64

Mader HM, Phillips JC, Sparks RSJ, Sturtevant B. 1996. Dynamics of explosive degassing of magma: observations of fragmenting two-phase flows. *J. Geophys. Res.* 101:5547–60

Mader HM, Zhang Y, Phillips JC, Sparks RSJ, Sturtevant B, Stolper EM. 1994. Experimental simulations of explosive degassing of magma. *Nature* 372:85–88

Maslin M, Mikkelsen N, Vilela C, Haq B. 1998. Sea-level and gas-hydrate-controlled catastrophic sediment failures of the Amazon Fan. *Geology* 26:1107–10

Mastin LG. 1995. A numerical program for steady-state flow of Hawaiian magma–gas mixtures through vertical eruption conduits. *U. S. Geol. Surv. Open-File Rep.*, pp. 95–156

Milgram JH. 1983. Mean flow in round bubble plumes. *J. Fluid Mech.* 133:345–76

Milkov AV. 2000. Worldwide distribution of submarine mud volcanoes and associated gas hydrates. *Mar. Geol.* 167:29–42

Morton BR, Taylor G, Turner JS. 1956. Turbulent gravitational convection from maintained and instantaneous sources. *J. R. Soc. London* A234:1–23

Murray CN, Riley JP. 1971. The solubility of gases in distilled water and seawater - IV. carbon dioxide. *Deep-Sea Res.* 18:533–41

Paull CK, Ussler W, Dillon W. 1991. Is the extent of glaciation limited by marine gas hydrate? *Geophys. Res. Lett.* 18:432–34

Phillips JC, Lane SJ, Lejeune AM, Hilton M. 1995. Gum rosin-acetone system as an analogue to the degassing behavior of hydrated magmas. *Bull. Volcanol.* 57:263–68

Rothwell RG, Thompson J, Kahler G. 1998. Low-sea-level emplacement of a very large late Pleistocene 'megaturbidite' in the western Mediterranean Sea. *Nature* 392:377–80

Ryskin G. 2003. Methane-driven oceanic eruptions and mass extinctions. *Geology* 31:741–44

Sabroux JC, Villevieille A, Dubois E, Doyotte C, Halbwachs M, Vandemeulebrouxk J. 1990. Satellite monitoring of the vertical temperature profile of Lake Nyos, Cameroon. *J. Volcanol. Geotherm. Res.* 42:381–84

Schmid M, Tietze K, Halbwachs M, Lorke A, McGinnis D, Wuest A. 2002/2003. How hazardous is the gas accumulation in Lake Kivu? Arguments for a risk assessment in light of the Nyiragongo volcano eruption of 2002. *Acta Vulcan.* 14/15:115–22

Shepherd JE, Sturtevant B. 1982. Rapid evaporation at the superheat limit. *J. Fluid Mech.* 121:379–402

Sigurdsson H, Devine JD, Tchoua FM, Presser TS, Pringle MKW, Evans WC. 1987. Origin of the lethal gas burst from Lake Monoun, Cameroon. *J. Volcanol. Geotherm. Res.* 31:1–16

Sigvaldason GE. 1989. International Conference on Lake Nyos Disaster, Yaoundé, Cameroon 16–20 March, 1987: conclusions and recommendations. *J. Volcanol. Geotherm. Res.* 39:97–107

Sloan ED. 1990. *Clathrate Hydrates of Natural Gases*. New York: Marcel Dekker. 641 pp.

Sparks RSJ, Bursik MI, Carey SN, Gilbert JS, Glaze LS, et al. 1997. *Volcanic Plumes*. New York: Wiley & Sons. 574 pp.

Tanyileke GZ, Kusakabe M, Evans WC. 1996. Chemical and isotopic characteristics of fluids along the Cameroon Volcanic Line, Cameroon. *J. Afr. Earth Sci.* 22:433–41

Tazieff H. 1989. Mechanisms of the Nyos carbon dioxide disaster and of so-called phreatic steam eruptions. *J. Volcanol. Geotherm. Res.* 39:109–16

Tietze K, Geyh M, Müller H, Schröder L, Stahl W, Wehner H. 1980. The genesis of methane in Lake Kivu (Central Africa). *Geol. Rundsch.* 69:452–72

Tsuchiya K, Furumoto A, Fan LS, Zhang J. 1997. Suspension viscosity and bubble rise velocity in liquid-solid fluidized beds. *Chem. Eng. Sci.* 52:3053–66

Turner JS. 1986. Turbulent entrainment: the development of the entrainment assumption, and its application to geophysical flows. *J. Fluid Mech.* 173:431–71

Walker GPL, Wilson L, Bowell ELG. 1971. Explosive volcanic eruptions—I. The rate of fall of pyroclasts. *Geophys. J. R. Astron. Soc.* 22:377–83

Weast RC. 1983. *CRC Handbook of Chemistry and Physics*. Boca Raton, FL: CRC Press

Weiss RF. 1974. Carbon dioxide in water and seawater: the solubility of a non-ideal gas. *Mar. Chem.* 2:203–15

Wilhelm E, Battino R, Wilcock RJ. 1977. Low-pressure solubility of gases in liquid water. *Chem. Rev.* 77:219–62

Wilson L. 1972. Explosive volcanic eruptions—II. The atmospheric trajectories of pyroclasts. *Geophys. J. R. Astron. Soc.* 30:381–92

Wilson L. 1976. Explosive volcanic eruptions—III. Plinian eruption columns. *Geophys. J. R. Astron. Soc.* 45:543–56

Wilson L, Sparks RSJ, Huang TC, Watkins ND. 1978. The control of volcanic column heights by eruption energetics and dynamics. *J. Geophys. Res.* 83:1829–36

Wilson L, Sparks RSJ, Walker GPL. 1980. Explosive volcanic eruptions—IV. The control of magma properties and conduit geometry on eruption column behavior. *Geophys. J. R. Astron. Soc.* 63:117–48

Woods A, Phillips JC. 1999. Turbulent bubble plumes and CO_2-driven lake eruptions. *J. Volcanol. Geotherm. Res.* 92:259–70

Woods AW. 1988. The dynamics and thermodynamics of eruption columns. *Bull. Volcanol.* 50:169–91

Woods AW. 1995. The dynamics of explosive volcanic eruptions. *Rev. Geophys.* 33:495–530

Zhang Y. 1996. Dynamics of CO_2-driven lake eruptions. *Nature* 379:57–59

Zhang Y. 1998. Experimental simulations of gas-driven eruptions: kinetics of bubble growth and effect of geometry. *Bull. Volcanol.* 59:281–90

Zhang Y. 2000. Energetics of gas-driven limnic and volcanic eruptions. *J. Volcanol. Geotherm. Res.* 97:215–31

Zhang Y. 2003. Methane escape from gas hydrate systems in marine environment, and methane-driven oceanic eruptions. *Geophys. Res. Lett.* 30(7):51–1–4, doi 10.1029/2002GL016658

Zhang Y. 2004. Mechanisms and dynamics of explosive volcanic and lake eruptions (in Chinese). In *Environment, Natural Hazards, and Global Tectonic of the Earth*, ed. Y Chen, pp. 39–95. Beijing: Higher Educ.

Zhang Y. 2005. Fate of rising CO_2 droplets in seawater. *Environ. Sci. Tech.* 39:7719–24

Zhang Y, Mader H, Brodsky E, Kanamori H, Kieffer S, et al. 2002. Bradford Sturtevant, 1933–2000. *Bull. Volcanol.* 63:569–71

Zhang Y, Sturtevant B, Stolper EM. 1997. Dynamics of gas-driven eruptions: experimental simulations using CO_2-H_2O-polymer system. *J. Geophys. Res.* 102:3077–96

Zhang Y, Sturtevant B, Stolper EM, Pyle D. 1992. Gas-powered volcanic eruptions. I. Preliminary results of experimental simulations on initiation of eruption, front advance and bubble growth. *Eos* 73F:628 (Abstr.)

Zhang Y, Xu Z. 2003. Kinetics of convective crystal dissolution and melting, with applications to methane hydrate dissolution and dissociation in seawater. *Earth Planet. Sci. Lett.* 213:133–48

Zimanowski B, Buttner R, Lorenz V, Hafele H-G. 1997. Fragmentation of basaltic melt in the course of explosive volcanism. *J. Geophys. Res.* 102:803–14

Annual Review of Earth and Planetary Sciences

Volume 34, 2006

Contents

INDEXES

ERRATA

An online log of corrections to *Annual Review of Earth and Planetary Sciences* chapters may be found at http://earth.annualreviews.org